# Strength and Nature of Hydrogen Bonding Interactions in Mono- and Di-Hydrated Formamide Complexes.

Emilio L. Angelina and Nélida M. Peruchena*

Laboratorio de Estructura Molecular y Propiedades, Área de Química Física, Departamento de Química, Facultad de Ciencias Exactas y Naturales y Agrimensura, Universidad Nacional del Nordeste, Avda. Libertad 5460, (3400) Corrientes, Argentina

ABSTRACT: In this work, mono- and di-hydrated complexes of the formamide were studied. The calculations were performed at the MP2/6-311++G(d,p) level of approximation. The atoms in molecules theory (AIM), based on the topological properties of the electronic density distribution, was used to characterize the different types of bonds. The analysis of the hydrogen bonds (H-bonds) in the most stable mono- and di-hydrated formamide complexes shows a mutual reinforcement of the interactions, and some of these complexes can be considered as "bifunctional hydrogen bonding hydration complexes". In addition, we analyzed how the strength and the nature of the interactions, in mono-hydrated complexes, are modified by the presence of a second water molecule in di-hydrated formamide complexes. Structural changes, cooperativity, and electron density redistributions demonstrate that the H-bonds are stronger in the di-hydrated complexes than in the corresponding mono-hydrated complexes, wherein the σ- and π-electron delocalization were found. To explain the nature of such interactions, we carried out the atoms in molecules theory in conjunction with reduced variational space self-consistent field (RVS) decomposition analysis. On the basis of the local Virial theorem, the characteristics of the local electron energy density components at the bond critical points (BCPs) (the $1/4\nabla^2\rho_b$ component of electron energy density and the kinetic energy density) were analyzed. These parameters were used in conjunction with the electron density and the Laplacian of the electron density to analyze the characteristics of the interactions. The analysis of the interaction energy components for the systems considered indicates that the strengthening of the hydrogen bonds is manifested by an increased contribution of the electrostatic energy component represented by the kinetic energy density at the BCP.
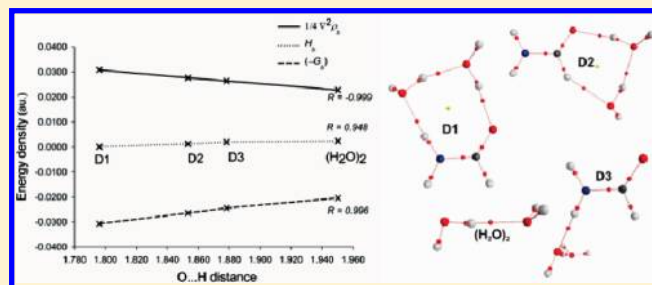
1. INTRODUCTION

In complex biological systems, the H-bonds may operate simultaneously, giving rise to interesting cooperativity effects among them. As is well-known, when they occur simultaneously, the collective strength of the set of H-bonds is larger than the sum of the individual bonds strength.[1−3] Jeffrey et al.[4] pointed out that there are two types of cooperativity: π-cooperativity, which is related to the π-electron delocalization in the resonance-assisted hydrogen bond (RAHB), and σ-cooperativity, which is related to σ-bonds connected to each other within a chain or a cycle. Many theoretical works show the existence of cooperativity in a variety of systems, as, for example, in clusters[1,5] and chains[6] of water molecules, in which σ-cooperativity is involved, or in cyclic clusters[7] and linear chains[8] of formamide molecules, in which RAHB occurs. However, there are fewer studies in which σ- and π-delocalization (simultaneously existing in a molecular system) can generate cooperativity (as, for example, in formamide/water complexes). The energy-based definition of cooperativity has been traditionally used in the discussion of cooperative phenomena.[9,10] However, the effects of cooperativity can be manifested in properties other than the energetic. For example, in a previous work,[11] we have examined the cooperative effects implicated in bifunctional H-bonds in monohydrated six−membered

cycloether, where the water molecule plays a dual role as a proton acceptor and a proton donor within the framework of the AIM theory[12,13] and of the natural bond orbital (NBO) analysis.[14] We have found that different indicators of H-bond strength such as structural and spectroscopic data, electron charge density, population analysis, hyperconjugation energy, and charge transference consistently show significant cooperative effects in bifunctional H-bonds. Consequently, we conclude that because of the σ-electron delocalization, cycloether/H_2O complexes engaged by bifunctional H-bonds are more stable than complexes bound by conventional H-bonds.[11] In the same sense, the other significant molecule that can act as a proton donor/acceptor simultaneously is the formamide, wherein σ- and π-electron delocalization are involved. This molecule can be considered as the minimum building block of the backbone of proteins, and a many works have been written about it.[15]

In the latest decades, several complexes of the SWn type (where S and W are solute and water molecules, respectively, n is the number of water molecules, and $n \geq 1$) and the SmWn type (where $m \geq 1$ and $n \geq 1$) have been studied[1,16−24] to explore

molecular solvation. Additionally, several studies have been carried out on methanol—water clusters, $MmWn$.[1,25,26] Mandal et al.[1] have recently studied the structure, stability, and spectroscopic characteristics of H-bonded methanol—water clusters, $MmWn$ (where $m + n \leq 4$, $m = 0$—4, and $n = 0$—4), to understand the cooperative effect in those systems. They performed an NBO analysis and a reduced variational space self-consistent field (RVS) decomposition analysis.[27] Their results clearly show that cooperative polarization and cooperative charge transference, in methanol—water and methanol—methanol complexes, are responsible for the increase in stability.

Moreover, the Bader theory[12] is very useful for studying the nature of the H-bond interactions because it provides more precise quantitative measures to describe them.

Grabowski et al.[28] have analyzed the "possible covalent nature of N—H···O H-bonds in the formamide dimer and related systems", representing a wide spectrum of more-or-less covalent interactions. By an analysis of the interaction energy components (via Morokuma—like analysis), they have established[28—31] that the covalent character of the hydrogen bond is manifested by a markedly increased contribution of the delocalization term, E_{DEL}, relative to the electrostatic interaction energy, E_{EL}. Their results indicate that the E_{DEL}/E_{EL} ratio increases with the increasing of the H-bond strength.[31] The delocalization energy is often treated as such a term that reflects the importance of the covalent character of the interactions. They performed an analysis of the interaction energy components in conjunction with the analysis of the local energy density descriptors derived from the Bader theory, that is, the electronic H_b, potential V_b, and kinetic G_b energy densities at the H-bond BCP. The authors found a correlation among the H···Y distance, the delocalization/electrostatic ratio, and the $-V_b/G_b$ ratio. On the basis of this background, we considered it attractive to examine, using different indicators, the strengthening of the H-bonds (due to cooperativity) in di-hydrated formamide complexes, as compared to mono-hydrated ones, wherein bifunctional as well as conventional H-bonds are involved. Additionally, we want to inquire in the nature of this strengthening. In other words, whether the strengthening is due to an increase in the "covalency" of the H-bond interaction or, otherwise, is the result of the increase in the electrostatic contribution to the interaction energy. With this purpose, we decomposed the local electronic energy density, H_b, in two densities, $(-G_b)$ and $1/4\nabla^2\rho_b$, which can be connected to the electrostatic and the nonelectrostatic part, respectively, of the total interaction energy. Our results show that the strengthening of the H-bonds, in the studied systems herein, is due to an increase in the electrostatic contribution to the total interaction energy.

2. METHODS AND CALCULATIONS DETAILS

To explore the mono-hydrated structures of the formamide using their molecular electrostatic potential (MEP), we used the AGOA 2.0 program.[32] (See more details in ref 33.) These hydration structures were used as an initial guess for a full geometry optimization for all complexes in gas phase at the MP2/6-311++G(d,p) level. In the case of the di-hydrated structures, we did not perform an exhaustive search over the entire MEP, as in the mono-hydrated structures. Instead, we considered only four di-hydrated structures of the formamide to quantify the cooperativity. Geometrical variables were optimized using Berny's analytical gradient method.[34] All stationary points

were characterized as an energy minimum by calculating the Hessian matrix. The interaction energy corrected by the basis set superposition error (BSSE) (using the counterpoise method of Boys and Bernardi[35]) was calculated as the difference between the total energy of the complexes minus the sum of the energies of the isolated monomers, ΔE_t^{corr}. All of these electronic structure calculations were performed with the Gaussian 03 suite of programs.[36]

The cooperativity $(\Delta E_{coop})^{37}$ among the H-bond interactions was calculated using eq 1

$$\Delta E_{coop} = \Delta E_{trimer} - \sum \Delta E_{dimer} \qquad (1)$$

where ΔE_{trimer} is the interaction energy of the formamide dihydrated complexes (a trimer) and $\sum \Delta E_{dimer}$ is the sum of the interaction energies of the corresponding mono-hydrated complexes, the water dimer, or both.

The calculations of local topological properties of the electron charge density at the critical points as well as the display of the molecular graphs were performed with the AIM2000 package[38] with the electron density obtained at the same level. Also, an interaction energy component analysis was carried out with the RVS energy decomposition scheme,[27] implemented in the GAMESS quantum chemistry package.[39]

$$E_{es} + E_{ex} + E_{pl} + E_{ct} + E_{res} = \Delta E_{RVS} \qquad (2)$$

In this energy decomposition analysis (EDA), ΔE_{RVS} represents the total interaction energy, calculated at a Hartee—Fock level, without considering the deformation energy of the monomers. E_{es} is the electrostatic energy describing the Coulomb interaction between the charge distributions of undistorted monomers, E_{ex} is the exchange—repulsion energy due to the Pauli's exclusion principle, E_{pl} is the polarization term that describes the Coulomb interaction between the charge distributions of the distorted monomers, and E_{ct} corresponds to the charge transfer term between the monomers (also called delocalization energy term in the scheme of Morokuma). Finally, E_{res} represents the difference between the sum of the energy components and the ΔE_{RVS}. It must be small for a valid RVS analysis.

When the correlation energy, E_{MP2}, and the deformation energy, E_{def}, are added to ΔE_{RVS}, then ΔE_t^{corr} is obtained. E_{MP2} is calculated as the difference between the MP2 and the Hartee—Fock interaction energies, both computed without considering the monomers deformation (i.e., with the monomers in the complex geometry). Then, E_{def} is calculated as the difference between the monomers energy in the complex and their isolated geometries,[40] both computed at the MP2 level.

In addition, the contribution of the interaction energy components E_{es}, E_{ex}, E_{pl}, E_{ct}, and ΔE_{RVS} to the cooperativity was computed by employing eq 1.

Besides the mono-hydrated and di-hydrated formamide complexes, a set of substituted formamide mono-hydrated complexes with a single H-bond interaction were studied, in which the H*cis* bonded to the nitrogen of the formamide molecule was replaced by X = $-CH_3$, $-NH_2$, $-F$, $-NO$, and $-CN$. This set of systems allowed us to study the variation of the RVS energy components and the AIM local energy densities as a function of the H-bond distance and to find a relationship between the local energy densities and the energy components of the RVS scheme.

The Results and Discussion section is organized as follows. In Section 3.1, a geometric, energetic, and charge density analysis of the mono-hydrated and di-hydrated formamide complexes was
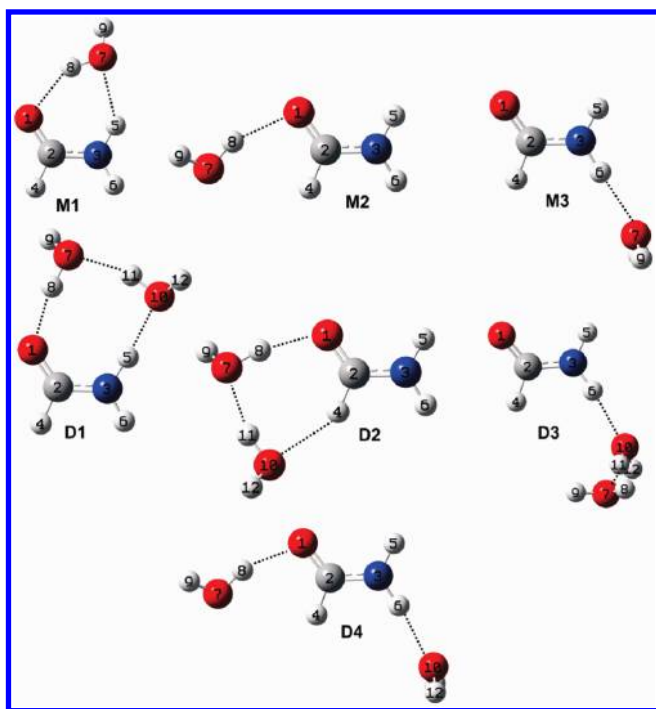
Figure 1. Optimized geometry for formamide/water complexes. Letter **M** denotes the mono-hydrated complexes and letter **D** denotes the di-hydrated complexes. The ordering numbers denote the stability of the complexes from the most stable (**M1** and **D1** to the least stable (**M3** and **D4**).

carried out to evaluate the strength of the H-bond interactions and the cooperativity effects. In Section 3.2, the RVS interaction energy components in the mono-hydrated and di-hydrated formamide complexes were analyzed. In Section 3.3, an equation to decompose H_b in two energy densities, $1/4\nabla^2\rho_b$ and $(-G_b)$, was derived. In Section 3.4, a set of substituted mono-hydrated formamide complexes were employed to relate the $1/4\nabla^2\rho_b$ and $(-G_b)$ energy densities to the energy components of the RVS scheme. Finally, at the end of Section 3.4 the proposed decomposition of H_b was tested in the mono-hydrated and di-hydrated formamide complexes.

3. RESULTS AND DISCUSSION

3.1. Geometric, Energetic, and Electron Charge Density Analysis. In Figure 1, the optimized geometries of mono- and di-hydrated formamide complexes (denoted as **M1**−**M3** complexes and **D1**−**D4** complexes, respectively) are shown. In this Figure, two different patterns of H-bonded monohydrated complexes can be seen. In **M1**, the water molecule and the formamide molecule itself play a dual role as a proton acceptor and as a proton donor; in **M2** and **M3**, the formamide (water) molecule simply acts as a proton acceptor (donor) or proton donor (acceptor), respectively. Similarly, as can be seen in Figure 1, **D1** and **D2** di-hydrated complexes form cyclic structures, wherein the formamide and the two water molecules act as proton donors as well as proton acceptors, but a different pattern of H-bonds is observed in the noncyclic structures (**D3** and **D4** complexes).

Table 1 shows MP2 results obtained with the 6-311++G(d,p) basis set for total interaction energy corrected by BSSE, (ΔE_t^{corr}). This table also reports relevant geometrical parameters, such as H-bond distances, H-bond angles, the proton

donor bond distances, and the CN and CO bond distances involved in π-electron delocalization (due to strong $n_N \rightarrow \pi^*C=O$ interaction).[41,42] In addition, data of the water dimer and formamide molecule are included. As can be seen in Table 1, the calculated ΔE_t^{corr} energies lie between −4.77 and −7.85 kcal/mol in mono-hydrated complexes and are of higher magnitude (from −10.82 to −16.98 kcal/mol) in di-hydrated complexes. These interaction energies increase in the order **M3** < **M2** < **M1** and **D4** ≈ **D3** < **D2** < **D1**, respectively. As expected, an increase in the stability is produced by the addition of a second water molecule. In all cases, a shorter H-bond distance in the di-hydrated relative to the mono-hydrated complexes is observed. In the di-hydrated complexes, as in the mono-hydrated complexes, the formation of cyclic structures provides the greatest stabilization of the complexes. The more stable di-hydrated complex has recently been observed by microwave spectroscopy in the gas phase.[15]

Figure 2 shows the molecular graphs of the three mono-hydrated and the four di-hydrated complexes analyzed in the present work. Also, the molecular graphs of the water dimer, the formamide, and the isolated water molecules are shown. The values of charge density at the BCP, ρ_b, in the interactions involved in the stabilization of the complexes are also included. The most stable mono-hydrated conformer of formamide, (**M1**), displays two strong contacts between the formamide and a single water molecule, which explains why this particular one has the highest stability among the three monohydrated complexes. In effect, the **M1** complex, which adopts a closer planar ring structure, is stabilized by a bifunctional hydrogen bond (i.e.; N−H*cis*···O(H)−H···O=C), whereas the water molecule acts as a Lewis acid (giving a proton to the oxygen atom of the carbonyl group) as well as a Lewis base (accepting a proton from the cis hydrogen of the amino group). This structure shows an agreement with the data reported by Lovas et al.[43] and recently by Blanco et al.[15] In this last paper, the authors[15] reported the two highest energy forms of formamide/H_2O complexes (**M2** and **M3**) using microwave spectroscopy with Fourier transform, which have never been experimentally observed before. The second most stable conformer (**M2**) is stabilized by a single HO−H···O=C hydrogen bond, wherein the trans lone pair (with respect to the N−C bond) is involved in the H−bond. In the less stable complex (**M3**), the water oxygen atom acts as a single proton acceptor of the anti hydrogen of the amino group of the formamide.

The comparison of H-bond distances and bond angles corresponding to the HO−H···O=C in **M2** and N−H···OH₂ H-bonds in **M3** complexes with similar interactions in **M1** complex shows that these individual contacts are stronger than those in the complex engaged by a bifunctional hydrogen bond. Table 1 illustrates how both isolated interactions show lower intermolecular distances (i.e., 1.930 in **M2** vs 1.952 Å in **M1** and 2.001 in **M3** vs 2.060 Å in **M1** structures) and how bond angles deviate less from colinearity. These structural results are a consequence of the **M1** cyclic structure, wherein some angular stress can be observed. (Note that the lone pair on the oxygen of the C=O group of the formamide, which acts as a proton acceptor, has a cis(trans) configuration with respect to the N−C bond of the FD in **M1**(**M2**) complexes.) Nevertheless, because of the two interactions present in **M1** complex, the charge density summation (considering both intermolecular BCPs) is higher (i.e., $\Sigma\rho_b = 0.0441$ au) than the intermolecular charge density in both isolated interactions, evaluated at

Table 1. Geometric and Energetic Parameters of the Mono-Hydrated and Di-Hydrated Formamide Complexes[a]

parameters	FD–H$_2$O			FD–(H$_2$O)$_2$				monomer	(H$_2$O)$_2$
	M1	M2	M3	D1	D2	D3	D4		
$\Delta E_t^{corr\,b}$	−7.85	−5.52	−4.77	−16.98	−13.47	−10.82	−10.83		−4.45
$d(C_2{=}O_1)^c$	1.226	1.223	1.221	1.230	1.229	1.222	1.228	1.217	
$d(N_3–C_2)$	1.356	1.360	1.358	1.348	1.357	1.358	1.351	1.364	
$d(N_3–H_5)$	1.015	1.009	1.008	1.023	1.009	1.009	1.009	1.008	
$d(N_3–H_6)$	1.006	1.007	1.011	1.007	1.007	1.015	1.013	1.006	
$d(O_7–H_8)$	0.971	0.968	0.960	0.976	0.975	0.961	0.970	0.959^d	0.961
$d(O_{10}–H_{11})$				0.976	0.972	0.969	0.961		0.966
$d(O_1{\cdots}H_8)$	1.952	1.930		1.811	1.831		1.889		
$d(H_{5,6}{\cdots}O_{7,10})$	2.060		2.001	1.888		1.939	1.978		
$d(O_{7,10}{\cdots}H_4)$		2.749			2.280				
$d(O_7{\cdots}H_{11})$				1.796	1.853	1.878			1.950
$\theta(O_1{\cdots}H_8–O_7)^e$	147.1	155.4		169.1	164.7		161.2		
$\theta(N_3–H_{5,6}{\cdots}O_{7,10})$	138.3		177.2	173.3		172.1	174.6		
$\theta(O_7{\cdots}H_{11}–O_{10})$				159.9	162.0	175.0			
$\theta(O_{7,10}{\cdots}H_4–C_2)$		101.5			150.4				

[a] Monomers and the water dimer are included. [b] ΔE_t^{corr}: total interaction energy corrected by BSSE in kilocalories per mole. [c] Bond distances in angstroms. [d] In isolated water. [e] Bond angles in degrees.

corresponding BCPs, $(\rho_{b(C{=})O{\cdots}H} = 0.0256$ au$)$ in **M2** and $(\rho_{b\,O{\cdots}H(N)} = 0.0204$ au$)$ in **M3** complexes. In consequence, becaue of the electron redistribution in the cyclic structure, the **M1** complex engaged by a bifunctional hydrogen bond results in the most stable mono-hydrated complex. In line with this observation, a lengthening in the O−H and N−H proton donor bonds was found. In general, the lengthening of the proton donor bond correlates well with the reduction of the H-bond distance; however, in the monohydrated complexes, this correlation is not observed. In other words, in bifunctional H-bond (**M1** complex), the enlargement of the O−H and N−H proton donor bonds is higher than in conventional H-bond (in **M2** and **M3** complexes). Despite this, the H-bond distances in **M1** are also higher. We believe that this is a characteristic of cyclic bifunctional H-bonds, wherein a significant electronic redistribution, due to polarization, is found. As expected, the lengthening of the donor bond was foremost in (**M1** and **D1**) complexes engaged by bifunctional H-bonds. Besides, a decrease in the electron charge density at the proton donor bond BCP, with respect to the isolated monomer, is always observed. (See Figure 2.) Our structural and energetic results are in agreement with those reported (in previous experimental and theoretical studies[15,44,45]) by other authors.

Cooperative Effects. To evaluate cooperativity possible existence, we compared the H-bond interactions in the di-hydrated complexes with similar ones in mono-hydrated complexes and in the water dimer.[37] Table 2 shows the energetic contribution due to cooperativity, ΔE_{coop}, as well as the percentage of interaction energy due to cooperativity, % coop. The energy gained in di-hydrated complexes (estimated as the difference between the E_{trimer} and the sum of E_{dimers}) lies in the range of 0.53 to 4.67 kcal/mol. Table 2 also indicates which mono-hydrated complexes (together with the water dimer) were taken into account, in each case, to calculate the cooperative effect. (See the last column.)

The results in Table 1 show that the two cyclic hydrated structures bonded by two water molecules, denoted by **D1** and **D2**, are more stable because of the formation of three hydrogen bonds, whereas the open structures (**D3** and **D4**) show only two intermolecular interactions. The first di-hydrated cyclic complex (**D1**) is more stable than the second complex, (**D2**), by 3.5 kcal/mol, and this result is not a surprise, considering that the N−H$_{cis}$$\cdots$OH$_2$ secondary interaction is more stabilizing than the C−H$_{gem}$$\cdots$OH$_2$ interaction. In the **D3** complex, a chain of two water molecules is associated with the N−H$_{trans}$ bond of the formamide molecule. This is the only one structure of hydration where the C=O group is not directly involved in an H−bond.

Another hydrogen bonding pattern is found in **D4** complex wherein the two water molecules are bonded to different sites of the formamide molecule without direct connection between them. In this complex the two O$\cdots$H H-bond distances are shorter than in **M2** and **M3** complexes and the N−H/O−H proton donor bond distances are longer.

Electron Charge Density Redistribution. When the interactions identified in **D1** are compared with similar interactions in **M1** and in the water dimer, (H$_2$O)$_2$, it is evident that the OH$\cdots$O H-bond shows an increase in the charge density at the corresponding BCP (by 28%), similarly, in the NH$\cdots$O H-bond (by 47.5%) and in the water bridge at the H$\cdots$O BCP (by 46%). In addition, an electron charge density redistribution is observed at the CN and CO covalent bonds (an augment of ρ_b in the first one and a decrease in the last one), accomplished by changes in the ellipticity values in both bonds. The reinforcement of the H-bonds in **D1** generates an additional stabilization of this complex; the cooperation calculated from eq 1 is ∼28%.

In addition, by comparison of ρ_b values at the same donor bond, it can be seen that the density decreases by complex formation following the expected order. $|\Delta\rho_b|$ (considered as the difference with respect to the same bond in the isolated molecule, in absolute value), at O−H donor bond, is higher in **D1** (0.0240 au) than in **M1** (0.0159 au), and the decrease in ρ_b at N−H donor bond is 0.0138 and 0.0060 au, respectively.

Similar changes or characteristics are observed in **D2** relative to **M2** and (H$_2$O)$_2$. In the first one, the increase observed at the HOH$\cdots$O(=C) BCP is 24%, and the reinforcement of the
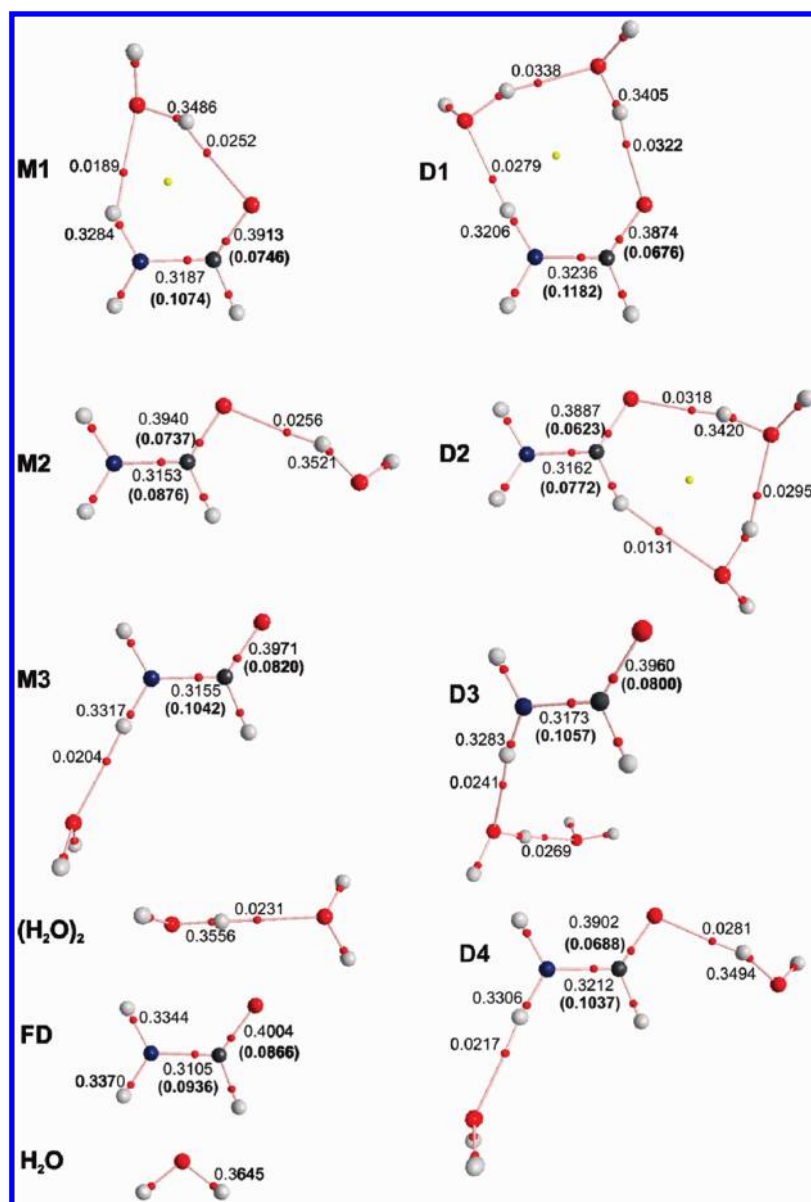
Figure 2. Molecular graphs for mono-hydrated and di-hydrated formamide complexes. Also, the water dimer and the monomers are included. Big circles correspond to attractors or nuclear critical point $(3, -3)$, attributed to nuclei; lines connecting the nuclei are the bond paths, and the small red circles on them are the bond critical points or $(3, -1)$ critical points. The small yellow circles are ring critical points or $(3, +1)$ critical points. The electronic charge density value (in au.) in selected BCPs is indicated. Additionally, the elipticity at the C=O and C−N BCPs is indicated in brackets.

Table 2. Energetic Contribution Due to the Cooperativity, ΔE_{coop}, in Di-Hydrated Formamide Complexes[a]

complexes	ΔE_{coop}[b]	% coop[c]	dimers
D1	−4.67	28	**M1** + $(H_2O)_2$
D2	−3.49	26	**M2** + $(H_2O)_2$
D3	−1.59	15	**M3** + $(H_2O)_2$
D4	−0.53	5	**M2** + **M3**

[a] Also, the dimers involved in the calculus of the cooperativity are shown. (See eq 1.) [b] ΔE_{coop} in kilocalories per mole. [c] % coop: percentage of the energetic contribution due to cooperativity.

HOH···OH$_2$ H-bond at the water bridge is marked by the increase in ρ_b (by 28%) relative to the same H···O BCP at the water dimer. Additionally, in **D2**, the incorporation of a second

water molecule makes possible the formation of a new H-bond with the hydrogen of the C−H bond. The cooperative effect in this trimer with respect to the corresponding dimers (**M2** and $(H_2O)_2$) is of 26%. (See Table 2.) Furthermore, a strengthening and a weakening of the CN and the CO covalent bonds (by ρ_b values) are also observed. These previously mentioned aspects, more important in **D1**, are indicative of an electron charge density shift due to a strong $n_N \rightarrow \pi^* C=O$ interaction that stretches and weakens the C=O bond.[42]

A different H-bond pattern is observed in the noncyclic structures (**D3** and **D4** complexes). In the first one, it can be observed that a water molecule acts as a bridge between the formamide and the water molecules (i.e., N−H$_{trans}$···O-(H)H···OH$_2$). The strengthening of the H-bonds can be valued by the augment of the charge density at the H$_{trans}$···O

4705

dx.doi.org/10.1021/jp1105168 |*J. Phys. Chem. A* 2011, 115, 4701–4710

Table 3. Interaction Energy Components from the RVS Method in the Mono- and Di-Hydrated Formamide Complexes[a,b]

complexes	components of the interaction energy						
	E_{es}	E_{ex}	E_{pl}	E_{ct}	ΔE_{RVS}	E_{MP2}	E_{def}
D1	−38.19	33.00	−6.48	−4.72	−17.25	−0.58	0.85
	(−11.48)	(12.49)	(−3.40)	(−2.07)	(−5.13)		
D2	−29.42	24.00	−4.66	−3.45	−14.07	0.21	0.39
	(−8.63)	(8.91)	(−2.47)	(−1.39)	(−4.01)		
D3	−21.95	16.32	−2.92	−1.82	−10.56	−0.39	0.13
	(−3.39)	(3.67)	(−1.08)	(−0.51)	(−1.44)		
D4	−21.57	15.73	−2.79	−2.13	−11.00	−0.07	0.24
	(−1.26)	(1.61)	(−0.56)	(−0.30)	(−0.62)		
M1	−17.19	13.73	−2.18	−1.88	−7.72	−0.33	0.20
M2	−11.27	8.28	−1.29	−1.29	−5.66	0.14	0.00
M3	−9.04	5.84	−0.94	−0.54	−4.72	−0.14	0.09
(H$_2$O)$_2$	−9.52	6.81	−0.90	−0.77	−4.40	−0.08	0.03

[a] In kilocalories per mole. [b] Contributions from each component to the cooperativity are indicated in parentheses. The correlation energy, E_{MP2}, and the deformation energy, E_{def}, are also shown.

BCP (0.0037 au greater than in **M3**, 18%). In addition, the increase in the electron charge density at the H···O BCP, due to the formation of a bridge between the water molecules, is 0.0068 au relative to (H$_2$O)$_2$ (16%). The strengthening of both interactions is due to the increase in the capacity as a Lewis acid as well as a Lewis base of the bridge water molecule in its role as a proton donor/acceptor. These cooperative effects are called by some authors as σ-cooperativity.[4,46] The increase in the energy stabilization in **D3** due to σ-electron reorganization is 1.59 kcal/mol, and the percentage of cooperativity is 15%.

D4 structure shows two H-bonds at two different H−bonding positions of the formamide, as proton acceptor at the carbonylic oxygen atom as well as a proton donor at the N−H$_{trans}$ bond from the amino group. The first one (i.e., HO−H···$_{trans}$O=C interaction) makes the NH group a better Lewis acid and reinforces the N−H$_{trans}$···OH$_2$ H-bond with respect to the **M3** complex (by 6.3%). Simultaneously, the formation of this H-bond in complex **D4** reinforces the HO−H···$_{trans}$O=C interaction with respect to the mono-hydrated **M2** complex (by 9.8%). In other words, when both interactions occur simultaneously they result mutually reinforced. In **D4** complex, the electron displacement is augmented by the effect of the two water molecules attached to both sides of the formamide molecule. It produces shortening/lengthening and strengthening/weakening of the CN/C=O bonds with an increase/decrease of the electron density at the BCPs. In turn, the π-electron delocalization acts by strengthening the (C=)O···H and NH$_{trans}$···O H-bonds.

Interestingly, the cooperative effect in the **D3** complex is almost three times the one found in **D4**. This reflects the higher contribution of the σ-electron delocalization to the cooperativity effect, in the **D3** complex, than the contribution of the π-electron delocalization to cooperativity in the **D4** complex.

3.2. Analysis of the Total Interaction Energy Components by RVS Scheme. The usefulness of the EDA based on reduced variational space self-consistent field scheme has been recognized in previous studies about the H-bond.[1,47,48] Consequently, to evaluate the various energetic contributions to the cooperativity,

an EDA analysis was performed using the RVS method. Table 3 shows the different components of the RVS total interaction energy (ΔE_{RVS}) in the mono- and di-hydrated formamide complexes. The contributions to the cooperativity are also included. In general, it can be observed that E_{es} and E_{ex} values are of higher magnitude than E_{pl} and E_{ct} and that the E_{MP2} and E_{def} values are small. In addition, $|E_{es}| > |E_{ex}|$ and $|E_{pl}| > |E_{ct}|$, in all complexes, with the exception of **M2** complex, wherein $|E_{pl}|$ and $|E_{ct}|$ show the same value.

From the data in Table 3, it can be observed that as the ΔE_{RVS} increases, the three stabilizing terms, that is, electrostatic, polarization, and charge transfer energy terms also increase in magnitude. This trend is fulfilled by all mono- and di-hydrated formamide complexes, except for the **D4** complex, in which the interaction energy components E_{es}, E_{ex}, and E_{pl} are lower in magnitude than in the **D3** complex, although the ΔE_{RVS} value in **D4** is slightly bigger in magnitude than in **D3** because of the E_{ct} term (which is 0.31 kcal/mol bigger in magnitude in **D4** than in **D3**).

Regarding the contribution of the various components of the interaction energy (in parentheses in Table 3) to the cooperativity, when only the stabilizing contributions are considered (i.e., from E_{es}, E_{pl}, and E_{ct}), the electrostatic term contributes to the cooperativity in about 68, 69, 68, and 60% in the **D1**, **D2**, **D3**, and **D4** di-hydrated complexes, respectively, whereas the polarization term contributes to the cooperativity in 20, 20, 22, and 26% and the charge transfer term in 12, 11, 10, and 14% in the **D1**, **D2**, **D3** and **D4** complexes, respectively. Therefore, these data indicate that the E_{es} and E_{pl} terms are the dominant contributions to the cooperativity in all di-hydrated complexes.

However, it is not possible to relate these results to a particular H-bond interaction because in the di-hydrated formamide complexes there is more than one H-bond and different binding patterns. In other words, like other global approaches to decompose the interaction energy into its various components, the RVS scheme does not give information about the individual interactions, when complexes with more than one H-bond interaction are considered. Moreover, in the context of the AIM theory, the local properties of the charge density, specifically the local energy density descriptors, are usually used to study the nature: electrostatic (closed shell interaction) or covalent (shared interaction), of the individual H-bond interactions.[28−31,47,49]

3.3. Analysis of the Local Energy Densities at the H-Bond BCP by AIM Method. In the AIM framework, the local statement of the virial theorem[12] provides a way to obtain the local energy densities from a property of the charge density as is its Laplacian, $\nabla^2\rho(r)$. The local statement of the virial theorem is (in au)

$$1/4\nabla^2\rho(r) = 2G(r) + V(r) \qquad (3)$$

The first term, $1/4\nabla^2\rho(r)$ (evaluated at the r point), represents the excess of energy density between two times the kinetic energy density, $G(r)$, and the potential energy density, $V(r)$.

Because $G(r) > 0$ and $V(r) < 0$, the potential energy is dominant in those space regions with electronic charge concentration where $\nabla^2\rho(r) < 0$, whereas the kinetic energy is dominant in regions where $\nabla^2\rho(r) > 0$. Therefore, a positive $\nabla^2\rho(r)$ at the BCP (i.e., $\nabla^2\rho_b$) reveals that the local contribution of the kinetic energy is greater than that of the potential energy and shows a depletion of the electronic charge along the bond path. This is the case encountered in closed shell (electrostatic) interactions.[12]

Moreover, the total electronic energy density function at the r point, $H(r)$, is related to $G(r)$ and $V(r)$ by the equation

$$H(r) = G(r) + V(r) \qquad (4)$$

On the basis of the classification of bonds proposed by Bader and Essén[50a] and Cremer and Kraka;[50b] bonds with a noncovalent character must have a BCP with positive values of $\nabla^2\rho(r)$ and $H(r)$. However, on the basis of the classification of Espinosa et al.,[51] the condition in which $|V(r)|/G(r) > 1$ but $|V(r)| < 2G(r)$ gives such a result where $\nabla^2\rho(r)$ would be positive (closed shell interaction), whereas $H(r)$ will still be negative (shared interaction). Therefore, they are generally termed as partially covalent and partially electrostatic bonds.[51,52] Nevertheless; it is known that typical hydrogen bonds that are in line with the Pauling's

Figure 3. Variation of $1/4\nabla^2\rho_b$, $(-G_b)$ and the H_b energy densities as a function of $(O \cdots H)$ H-bond distance between the two water molecules (in angstoms).The correlation coefficients, R, and the equations of the linear regressions are included. The data shown correspond to **D1**, **D2**, and **D3** di-hydrated complexes and the water dimer, $(H_2O)_2$.

definition of hydrogen bonding are mostly electrostatic in nature, with positive values for terms $\nabla^2\rho_b$ and H_b.

Reordering eq 3, we can write another equation where we get two alternative expressions for the local electronic energy density, $H(r)$.

$$1/4\nabla^2\rho(r) + (-G(r)) = G(r) + V(r) = H(r) \qquad (5)$$

We expressed these quantities in atomic units. The second member of eq 5 is the usual form to decompose $H(r)$, same as in eq 4, whereas in the first member, the total electronic energy density at the BCP is decomposed in two different energy densities contributions, $1/4\nabla^2\rho(r)$ and $(-G(r))$. From now on, we have changed the subscript (r) to b to indicate that local properties are measured at the BCP.

As is shown in Section 3.1, the reinforcement of the individual H-bond interaction by the addition of a second water molecule (i. e., from the mono-hydrated to the di-hydrated formamide complexes) is due to the cooperative effects among the H-bond interactions. The electronic charge density values at the H-bond BCP (ρ_b) between the two water molecules properly describes this strengthening. However, to inquire about the nature of this H-bond, local energy density descriptors are needed.

In Figure 3, the variations of $1/4\nabla^2\rho_b$, $(-G_b)$, and the H_b energy densities are represented as a function of $(O \cdots H)$ H-bond distances between the two water molecules in **D1**, **D2**, and **D3** di-hydrated complexes. The values for $(H_2O)_2$ are also depicted. The values of the correlation coefficients ($R = -0.999$ for $1/4\nabla^2\rho_b$ and $R = 0.996$ for $(-G_b)$) show that the lineal correlation of both energy densities with the $H \cdots O$ distance is even better than the lineal correlation of ρ_b with the $H \cdots O$ distance ($R = 0.992$, results not shown). This Figure shows that the term $1/4\nabla^2\rho_b$ increases with the decrease in the $H \cdots O$ distance, or, in other words, with the increase in the strength of the interaction. In the same way, $(-G_b)$ increases in magnitude
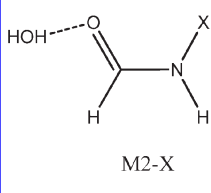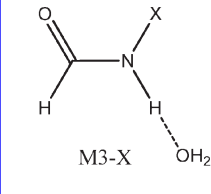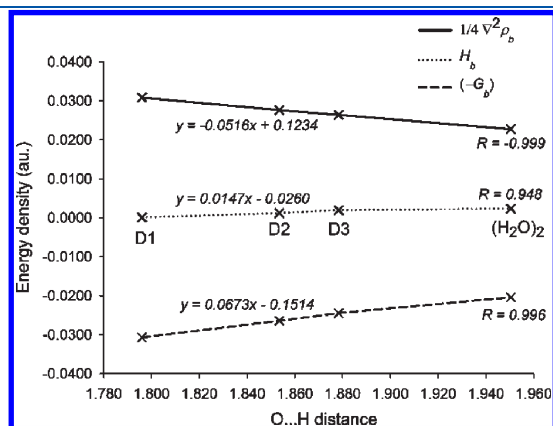
Table 4. Interaction Energy Components from the RVS Scheme and Energy Densities from AIM Method as a Function of $(O \cdots H)$ H-Bond Distance in Substituted M2 and M3 Monohydrated Complexes

Complexes	X	$d(O \cdots H)^a$	RVS energy decomposition[b]						AIM energy density decomposition[c]		
			E_{cs}	E_{ex}	E_{pl}	E_{ct}	E_{res}^d	ΔE_{RVS}^e	$1/4\nabla^2\rho_b$	H_b	$(-G_b)$
M2-X	CH_3	1.907	−11.83	8.85	−1.41	−1.42	−0.10	−5.91	0.0245	0.0014	−0.0231
	H	1.930	−11.27	8.28	−1.29	−1.29	−0.09	−5.66	0.0235	0.0016	−0.0218
	NH_2	1.933	−11.16	8.28	−1.26	−1.28	−0.10	−5.52	0.0234	0.0016	−0.0218
	F	2.059	−9.37	6.28	−0.93	−0.92	−0.07	−5.01	0.0183	0.0019	−0.0164
	$N=O$	2.088	−9.14	5.98	−0.90	−0.86	−0.07	−4.99	0.0173	0.0018	−0.0155
	$C\equiv N^f$	2.115	−9.19	5.82	−0.88	−0.78	−0.06	−5.09	0.0164	0.0017	−0.0147
M3-X	CH_3	2.001	−8.81	6.06	−0.98	−0.53	−0.04	−4.30	0.0207	0.0025	−0.0182
	H	2.001	−9.04	5.84	−0.94	−0.54	−0.04	−4.72	0.0206	0.0026	−0.018
	NH_2	1.971	−9.55	6.92	−1.04	−0.70	−0.03	−4.40	0.0219	0.0022	−0.0197
	F	1.908	−12.65	8.54	−1.43	−1.03	−0.07	−6.64	0.0248	0.0018	−0.0230
	$N=O$	1.928	−12.58	8.36	−1.41	−0.94	−0.09	−6.66	0.0235	0.0018	−0.0217
	$C\equiv N$	1.861	−14.48	9.48	−1.72	−1.13	−0.11	−7.96	0.0271	0.0015	−0.0256

^{a} In angstroms. ^{b} In kilocalories per mole. ^{c} In au. ^{d} E_{res} must be small for a valid RVS analysis. ^{e} ΔE_{RVS} is the total interaction energy calculated at the HF/6-311++G(d,p)//MP2/6-311++G(d,p) level. ^{f} This substituted M2−complex differs from the others in that it presents two H-bond critical points at $C=O \cdots H−OH$ and at weak $C−H \cdots OH_2$ interactions. For this reason, ΔE_{RVS} is more negative than expected from the $O \cdots H$ distance.
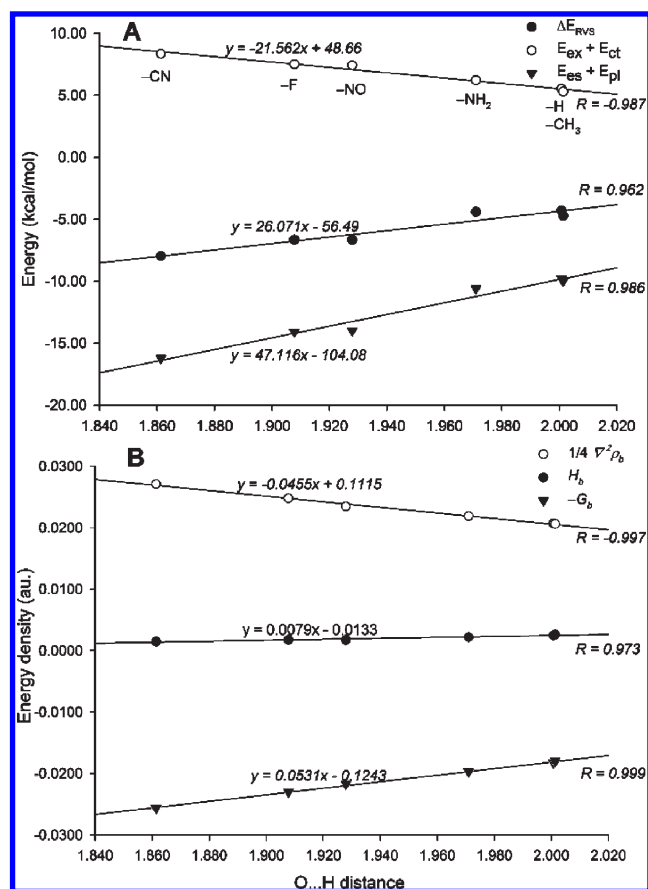
Table 5. $1/4\nabla^2\rho_b$, $(-G_b)$, and H_b Energy Densities At H-Bond Interactions in the Mono- and Di-Hydrated Formamide Complexes[a]

interactions	complexes	ρ_b	$1/4\nabla^2\rho_b$	H_b	$(-G_b)$
$N-H_{cis}\cdots OH_2$	D1	0.0279	0.0252	0.0013	−0.0239
	M1	0.0189	0.0189	0.0024	−0.0165
$N-H_{trans}\cdots OH_2$	D3	0.0241	0.0236	0.0023	−0.0213
	D4	0.0217	0.0217	0.0025	−0.0192
	M3	0.0204	0.0206	0.0026	−0.0180
$HO-H\cdots_{cis}O=C$	D1	0.0322	0.0291	0.0005	−0.0286
	M1	0.0252	0.0222	0.0013	−0.0209
$HO-H\cdots_{trans}O=C$	D2	0.0318	0.0279	0.0003	−0.0276
	D4	0.0281	0.0252	0.0012	−0.0240
	M2	0.0256	0.0235	0.0016	−0.0218
$HO-H\cdots OH_2$	D1	0.0338	0.0308	0.0000	−0.0308
	D2	0.0295	0.0276	0.0012	−0.0265
	D3	0.0269	0.0264	0.0019	−0.0245
	$(H_2O)_2$	0.0231	0.0228	0.0023	−0.0204

[a] ρ_b, $1/4\nabla^2\rho_b$, $(-G_b)$, and H_b are given in au.

Figure 4. (A) Correlation of (ΔE_{RVS}), $(E_{ct} + E_{ex})$, and $(E_{el} + E_{pl})$ terms with the $(O\cdots H)$ H-bond distance (in angstroms) in the substituted **M3** mono-hydrated complexes and (B) idem correlation of $1/4\nabla^2\rho_b$, $(-G_b)$, and H_b energy densities with the $(O\cdots H)$ H-bond distance. The correlation coefficient, R, and the equations of the linear regressions are included.

and H_b slowly diminish its positive values with the decrease in the $H\cdots O$ distance.

3.4. Relationships between the Local Energetic Parameters (AIM) and Energy Decomposition (RVS) with the $(O\cdots H)$ H-Bond Distance. In an attempt to relate the variation (with the decrease in the $H\cdots O$ H-bond distance) of the topological parameters derived from the Bader theory (i.e., the G_b values and the $1/4\nabla^2\rho_b$ values) with the variation of the components of the ΔE_{RVS} in the complexes studied here, an EDA analysis in several related systems that present a single H-bond interaction was carried out. In this form, the results of the RVS analysis can be directly related with a particular H-bond interaction. Then, substituted **M2** and **M3** mono-hydrated complexes (in which the H*cis* bonded to nitrogen of the formamide molecule was replaced by X = $-CH_3$, $-NH_2$, $-F$, $-NO$, and $-CN$) were considered. For each substituted complex: (i) the components of the total interaction energy, as in the partitioning of the RVS scheme (eq 2), and (ii) the local energy densities $1/4\nabla^2\rho_b$, $(-G_b)$ and H_b, were analyzed.

Table 4 shows that the $(O\cdots H)$ H-bond distance changes in an opposite order with the replacement in substituted **M2** and **M3**, denoted **M2−X** and **M3−X** complexes, respectively. In **M2−X** complexes, the $(O\cdots H)$ H-bond distance decrease following the order: $-C\equiv N$ > $-N=O$ > $-F$ > $-NH_2$ > $-H$ > $-CH_3$,

whereas in the **M3−X** complexes, the $(O\cdots H)$ H-bond distance decreases following nearly the opposite order: $-CH_3$ $\sim$ $-H$ > $-NH_2$ > $-N=O$ > $-F$ > $-C\equiv N$. The methyl group operates as the electron-donating substituent, and the $-N=O$, $-F$, $-C\equiv N$, and even the $-NH_2$ group (by inductive effect solely) can be considered to be electron-withdrawing substituents.

The opposite tendency in **M2−X** and **M3−X** complexes can be rationalized as follows. In **M2−X** complexes, the electron-withdrawing substituents weaken the interaction $nN \rightarrow \pi^*C=O$ via σ-bond polarization, π-delocalization, or both. In consequence, the Lewis base capacity of the carbonylic oxygen atom is reduced, and the $O\cdots H$ distance is enlarged. On the contrary, in the substituted **M3−X** complexes, the electron-withdrawing substituents polarize the adjacent N−H bond. As a result, the Lewis acid capacity of the N−H bond is increased and the $O\cdots H$ distance is shortened.

Going back to eq 2, the charge transfer energy, E_{ct}, is often treated as such a term that reflects the importance of the covalent character of the interactions.[31] Moreover, the positive term E_{ex} reflects the requirements of the Pauli exclusion principle. These two terms together $(E_{ex} + E_{ct})$ qualitatively describe the behavior of the $1/4\nabla^2\rho_b$ term for closed shell interactions. (A more/less positive value of $1/4\nabla^2\rho_b$ is associated with a more/less positive $(E_{ex}+E_{ct})$ sum.)

Moreover, the electrostatic (E_{es}) and the polarization (E_{pl}) components can be grouped in a single "electrostatic" term. As was expressed by Dannenberg et al.,[53] the "electrostatic" term applies to interactions between entities that have fixed electron densities, such as point charges. Often, also, the term is used to include polarization, which is not "static".[53] In addition, the polarization in the RVS scheme is expressed as associated with the "internal" redistribution of electron charge.[1]

Following, in Figure 4A,B, the energetic terms $(E_{ct} + E_{ex})$, $(E_{es} + E_{pl})$, and ΔE_{RVS}, and the local energy density terms $(1/4\nabla^2\rho_b$, $(-G_b)$ and $H_b)$ are represented as a function of the $H\cdots O$ distance in the **M3−X** complexes. In these Figures, a similar behavior between the term $1/4\nabla^2\rho_b$ in the AIM method and the quantity $(E_{ct} + E_{ex})$ in the RVS scheme, as a function of the

H···O distance, can be observed. Both terms show a smooth increase with the decrease in the H···O distance.

In addition, a similar tendency of variation can be observed between $(-G_b)$ and the electrostatic components of the RVS scheme, $(E_{es} + E_{pl})$, with the H···O distance. Furthermore, as can be seen from Figure 4A,B; ΔE_{RVS} as well as H_b decrease with the H···O distance, although the variation of H_b is smoother than the variation of ΔE_{RVS}. In other words, ΔE_{RVS} takes more negative values (by the increase in magnitude) with the decrease in the H···O distance, and H_b diminishes its positive value with the decrease in the H···O distance.

In summary, our results provide a different interpretation for H_b as a local electronic energy density that can be decomposed in two local energy densities, $(-G_b)$ and $1/4\nabla^2\rho_b$, which are connected with the $(E_{es} + E_{pl})$ and $(E_{ex} + E_{ct})$ terms of the ΔE_{RVS}, respectively.

In turn, the $(E_{es} + E_{pl})$ term can be related to the "purely electrostatic part" of the interaction, whereas the $(E_{ex} + E_{ct})$ term accounts for the "sharing of electrons" between the monomers.[54] Then, the interactions have more-or-less covalent character depending on the magnitude of E_{ct} relative to E_{ex}, as was explained above.

Having tested the proposed energy density decomposition (in M2−X and M3−X complexes) with the RVS scheme, we will apply it to the mono- and di-hydrated complexes. In several of these complexes, multiple H-bond interactions occur simultaneously, and a local analysis, as proposed here, is needed to carry out the EDA over the individual interactions.

Table 5 summarizes the values of the topological properties as charge density and the energy densities $(1/4\nabla^2\rho, (-G_b)$ and $H_b)$ evaluated at the BCP in the different interactions present in mono- and di-hydrated formamide complexes.

In all cases, the ρ_b values show that the H-bond interactions in di-hydrated complexes are stronger than the same interactions in mono-hydrated complexes. In line with these findings, the $1/4\nabla^2\rho_b$ and $(-G_b)$ energy densities also increase their magnitude in the same sense. In the previous discussion, we have associated or related the $1/4\nabla^2\rho_b$ term with the $(E_{ct} + E_{ex})$ term of the RVS decomposition. In consequence, we attribute the increase in $1/4\nabla^2\rho_b$ to an increase in the energy exchange (E_{ex} is always positive whereas E_{ct} is negative), where a more positive value of $1/4\nabla^2\rho_b$ is indicative of an increase in the interelectronic repulsion at the BCP, as can be expected in H-bond interactions, where the charge density is shifted from the atomic interaction surface toward the basin of each of the linked atoms. In addition, the $(-G_b)$ term was related to the electrostatic components $(E_{es} + E_{pl})$, and its increase (in absolute value) clearly indicates an increase in the electrostatic contribution to the interaction energy.

Simultaneously to this increase in the electrostatic component, the local electronic energy density, H_b, decreases in magnitude and takes the minor value in D1 complex. This trend of H_b toward negative values is generally attributed to the covalence of the interaction by other authors.[28−31,51,52] However, our results indicate that the decrease in H_b is a consequence of the increase in magnitude of the term $(-G_b)$ associated with the electrostatic energy, whose increase in magnitude is higher than the increase in $1/4\nabla^2\rho_b$ in the analyzed interactions.

4. CONCLUSIONS

A theoretical study about the mono- and di-hydrated complexes of the formamide was carried out at the MP2/6-311++G-(d,p) level of approximation. An energetic analysis, based on the local Virial theorem, in the context of the AIM theory, was related to the interaction energy components from the RVS analysis.

We have found that the cyclic structures (i.e.; M1 from the mono-hydrated and D1 and D2 from the di-hydrated complexes) can be described as bifunctional hydrogen bonding hydration complexes. They resulted more stabilized than the noncyclic structures. The energetic stabilization increases in the order: M3 < M2 < M1 and D4 ≈ D3 < D2 < D1, wherein several topological indicators of σ-electron and π-electron delocalization and subsequent cooperative effects were established.

The large percentage of the cooperation found in D1 and D2 structures (28 and 26%, respectively; against 15% in D3 and 5% in D4), is due to the incorporation of a second water molecule to the M1 and M2 structures. This relieves the angular tension in M1 and improves the colinearity of the interacting atoms as well as the redistribution of the electron density. Although D3 and D4 complexes have similar total interaction energies, the cooperative effects in D3 are three times higher than in D4. In the first one, the water bridge bonded to N−H of the formamide molecule produces a higher σ-electronic delocalization in the whole complex (σ-cooperativity). In contraposition, in the last complex, the higher π-delocalization exhibited by the formamide (bonded to two water molecules nonengaged between them) can be seen relative to the isolated formamide. Both electron delocalizations occur simultaneously in these hydration structures; however, the comparison of their features (in D3 and D4 complexes) indicates that the σ-cooperativity is quantitatively more significant than the π-delocalization. In line with these results, the polarization term is slightly higher in D3 (-2.92 kcal/mol) than in D4 (-2.74 kcal/mol), and the charge transference term is higher in D4 that in D3 (-2.13 vs -1.82 kcal/mol).

On the basis of the EDA, we have found that the electrostatic and the polarization components have significant contribution to the total interaction energy and, in contraposition, the correlation energy representing dispersion interaction does not play a crucial role in the stability of the hydration structures.

A linear relationship was established between the (H···O) H-bond distance between the two water molecules in the di-hydrated complexes and the local topological parameters ρ_b, $(-G_b)$, $(1/4\nabla^2\rho_b)$ and (H_b) at the BCPs. Furthermore, a good lineal correlation was established between the terms $1/4\nabla^2\rho_b$ ($R = -0.997$) and $(-G_b)$ ($R = 0.999$) energy densities with the (H···O) H-bond distance, in the M3−X complexes, indicating that these topological parameters can be considered as good local descriptors of the strength of these interactions. Similarly, lineal relationships among (ΔE_{RVS}), $(E_{ct} + E_{ex})$, and $(E_{el} + E_{pl})$ terms with the (H···O) H-bond distance were also established. In addition, energetic parameters derived from Bader's theory were related to the energetic decomposition terms provided by the RVS scheme. From the AIM theory as well as from the RVS analysis we conclude that the reinforcement of the H-bonds with the decrement of the (H···O) H-bond distance is due to a greater increment of kinetic energy density, in relation to the increment of the $(1/4\nabla^2\rho_b)$ energy density, which is also due to a greater increase in magnitude of the $(E_{el} + E_{pl})$ term in relation to the $(E_{ct} + E_{ex})$ term. That is to say, the strengthening of the hydrogen bonds in the studied systems herein is due to an increase in the electrostatic contribution to the total interaction energy.

■ AUTHOR INFORMATION

Corresponding Author
*E-mail: arabeshai@yahoo.com.ar.

■ REFERENCES

(1) Mandal, A.; Prakash, M.; Kumar, R. M.; Parthasarathi, R.; Subramanian, V. *J. Phys. Chem. A* **2010**, *114*, 2250.

(2) Parthasarathi, R.; Subramanian, V.; Sathyamurthy, N. *J. Phys. Chem. A* **2005**, *109*, 843.

(3) Ludwig, R. *Angew. Chem., Int. Ed.* **2001**, *40*, 1808.

(4) Jeffrey, G. A.; Saenger, W. *Hydrogen Bonding in Biological Structures*; Springer-Verlag: New York, 1991.

(5) Znamenskiy, V. S.; Green, M. E. *J. Chem. Theory. Comput.* **2007**, *3*, 103.

(6) Kar, T.; Scheiner, S. *J. Phys. Chem. A* **2004**, *108*, 9161.

(7) Cabaleiro-Lago, E. M.; Otero, J. R. *J. Chem. Phys.* **2002**, *117*, 1621.

(8) Kobko, N.; Paraskevas, L.; del Rio, E.; Dannenberg, J. J. *J. Am. Chem. Soc.* **2001**, *123*, 4348.

(9) Parra, R. D.; Furukawa, M.; Gong, B.; Zeng, X. C. *J. Chem. Phys.* **2001**, *115*, 6030.

(10) Parra, R. D.; Gong, B.; Zeng, X. C. *J. Chem. Phys.* **2001**, *115*, 6036.

(11) Vallejos, M. M.; Angelina, E. L.; Peruchena, N. M. *J. Phys. Chem. A* **2010**, *114*, 2855.

(12) Bader, R. F. W. *Atoms in Molecules: A Quantum Theory*; Oxford University Press: New York, 1994.

(13) Popelier, P. L. *Atoms in Molecules: An Introduction*; Prentice Hall: New York, 2000.

(14) Gledening, E. D.; Reed, A. E.; Carpenter, J. A.; Weinhold, F. *NBO*, version 3.1; University of Wisconsin: Madison, WI.

(15) Blanco, S.; López, J. C.; Lesarri, A.; Alonso, J. L. *J. Am. Chem. Soc.* **2006**, *128*, 12111.

(16) Nagaraju, M.; Narahari Sastry, G. *Int. J. Quantum Chem.* **2010**, *110*, 1994.

(17) Masella, M.; Flament, J. P. *J. Chem. Phys.* **1998**, *108*, 7141.

(18) Geronimo, I.; Chéron, N.; Fleurat-Lessard, P.; Dumont, É. *Chem. Phys. Lett.* **2009**, *481*, 173.

(19) Bachrach, S. M.; Nguyen, T. T.; Demoin, D. W. *J. Phys. Chem. A* **2009**, *113*, 6172.

(20) Michaux, C.; Wouters, J.; Perpète, E. a.; Jacquemin, D. *J. Phys. Chem. B* **2008**, *112*, 7702.

(21) Nguyen, M. T.; Matus, M. H.; Jackson, V. E.; Vu, T. N.; Rustad, J. R.; Dixon, D. A. *J. Phys. Chem. A* **2008**, *112*, 10386.

(22) Mejía, S. M.; Espinal, J. F.; Mondragón, F. *THEOCHEM* **2009**, *901*, 186.

(23) Mejía, S. M.; Espinal, J. F.; Restrepo, A.; Mondragón, F. *J. Phys. Chem. A* **2007**, *111*, 8250.

(24) Oliveira, B. G.; Vasconcellos, M. L. A. A. *THEOCHEM* **2006**, *774*, 83.

(25) Fileti, E. E.; Canuto, S. *Int. J. Quantum Chem.* **2005**, *102*, 554.

(26) Gonzàlez, L.; Mó, O.; Yàñez, M. *J. Chem. Phys.* **1998**, *109*, 139.

(27) Stevens, W. J.; Fink, W. H. *Chem. Phys. Lett.* **1987**, *139*, 15.

(28) Grabowski, S. J.; Sokalski, W. A.; Leszczynski, J. *J. Phys. Chem. A* **2006**, *110*, 4772.

(29) Grabowski, S. J.; Sokalski, W. A.; Dyguda, E.; Leszczyński, J. *J. Phys. Chem. B* **2006**, *110*, 6444.

(30) Gora, R. W.; Grabowski, S. J.; Leszczynski, J. *J. Phys. Chem. A* **2005**, *109*, 6397.

(31) Grabowski, S. J. *Croat. Chem. Acta* **2009**, *82*, 185.

(32) Hernandes, M. Z. *AGOA Program*, version 2.0; Depto. de Ciências Farmacêuticas (UFPE), Recife: Pernambuco, Brazil, 2003. http://www.ufpe.br/farmacia/zaldini/agoa.html.

(33) Oliveira, B. G.; Araújo, R. C. M. U.; Carvalho, A. B.; Ramos, M. N.; Hernandes, M. Z.; Cavalcante, K. R. *THEOCHEM* **2007**, *802*, 91.

(34) Schlegel, H. B. *J. Comput. Chem.* **1982**, *3*, 214.

(35) Boys, S. F.; Bernardi, F. *Mol. Phys.* **1970**, *19*, 553.

(36) Frisch, M. J.; Trucks, G. W.; Schlegel, H. B.; Scuseria, G. E.; Robb, M. A.; Cheeseman, J. R.; Montgomery, J. A., Jr.; Vreven, T.; Kudin, K. N.; Burant, J. C.; Millam, J. M.; Iyengar, S. S.; Tomasi, J.; Barone, V.; Mennucci, B.; Cossi, M.; Scalmani, G.; Rega, N.; Petersson, G. A.; Nakatsuji, H.; Hada, M.; Ehara, M.; Toyota, K.; Fukuda, R.; Hasegawa, J.; Ishida, M.; Nakajima, T.; Honda, Y.; Kitao, O.; Nakai, H.; Klene, M.; Li, X.; Knox, J. E.; Hratchian, H. P.; Cross, J. B.; Adamo, C.; Jaramillo, J.; Gomperts, R.; Stratmann, R. E.; Yazyev, O.; Austin, A. J.; Cammi, R.; Pomelli, C.; Ochterski, J. W.; Ayala, P. Y.; Morokuma, K.; Voth, G. A.; Salvador, P.; Dannenberg, J.J.; Zakrzewski, G.; Dapprich, S.; Daniels, A. D.; Strain, M. C.; Farkas, O.; Malick, D. K.; Rabuck, A. D.; Raghavachari, K.; Foresman, J. B.; Ortiz, J. V.; Cui, Q.; Baboul, A. G.; Clifford, S.; Cioslowski, J.; Stefanov, B. B.; Liu, G.; Liashenko, G. A.; Piskorz, P.; Komaromi, I; Martin, R. L.; Fox, D. J.; Keith, T.; Al-Laham, M. A.; Peng, C. Y.; Nanayakkara, A.; Challacombe, M.; Gill, P. M. W.; Johnson, B.; Chen, W.; Wong, M. W.; Gonzalez, C.; Pople, J. A. *Gaussian 03*, revision D.01; Gaussian, Inc.:Wallingford CT, 2004.

(37) Dannenberg, J. J. *J. Phys. Chem. A* **2006**, *110*, 5798.

(38) Biegler-König, F.; Schönbohn, J. *AIM2000 Program Package*, version 2.0; Buöro fur Innovative Software Streibel Biegler-König: Bielefeld, Germany, 2002 (Chemical advice by R. F. W. Bader).

(39) Schmidt, M. W.; Baldridge, K. K.; Boatz, J. A.; Elbert, S. T.; Gordon, M. S.; Jensen, J. H.; Koseki, S.; Matsunaga, N.; Nguyen, K. A.; Su, S.; Windus, T. L.; Dupuis, M.; Montgomery, J. A. *J. Comput. Chem.* **1993**, *14*, 1347.

(40) Cabaleiro-Lago, E. M.; Rodríguez Otero, J. *J. Chem. Phys.* **2002**, *117*, 1621.

(41) Fogarasi, G.; Szalay, P. G. *J. Phys. Chem. A* **1997**, *101*, 1400.

(42) (a) Beck, J. F.; Mo, Y. *J. Comput. Chem.* **2007**, *28*, 455. (b) Mo, Y.; Schleyer, P. v. R.; Wu, W.; Lin, M.; Zhang, Q.; Gao, J. *J. Phys. Chem. A* **2003**, *107*, 10011. (c) Glendening, E. D.; Hrabal, J. A. *J. Am. Chem. Soc.* **1997**, *119*, 12940. (d) Lauvergnat, D.; Hiberty, P. C. *J. Am. Chem. Soc.* **1997**, *119*, 9478.

(43) Lovas, F. J.; Suenram, R. D.; Fraser, G. T.; Gillies, C. W.; Zozom, J. *J. Chem. Phys.* **1988**, *88*, 722.

(44) Engdahl, A.; Nelander, B.; Åstrand, P. O. *J. Chem. Phys.* **1993**, *99*, 4894.

(45) Fu, A.; Du, D.; Zhou, Z. *THEOCHEM* **2003**, *623*, 315.

(46) Bertolasi, V.; Pretto, L.; Gilli, G.; Gilli, P. *Acta Crystallogr., Sect. B* **2006**, *62*, 850.

(47) Roohi, H.; Nowroozi, A. R.; Eshghi, F. *Int. J. Quantum Chem.* **2010**, *110*, 1489.

(48) Biswal, H. S.; Shirhatti, P. R.; Wategaonkar, S. *J. Phys. Chem. A* **2009**, *113*, 5633.

(49) Roohi, H.; Bagheri, S. *Int. J. Quantum Chem.* **2011**, *111*, 961.

(50) (a) Bader, R. F. W.; Essén, H. *J. Chem. Phys.* **1984**, *80*, 1943. (b) Cremer, D.; Kraka, E. *Angew. Chem., Int. Ed. Engl.* **1984**, *23*, 627.

(51) Espinosa, E.; Alkorta, I.; Elguero, J.; Molins, E. *J. Chem. Phys.* **2002**, *117*, 5529.

(52) Pakiari, A. H.; Eskandari, K. *THEOCHEM* **2006**, *759*, 51.

(53) Masunov, A.; Dannenberg, J. J.; Contreras, R. H. *J. Phys. Chem. A* **2001**, *105*, 4737.

(54) We want to emphasize that there is a significant difference, from the chemical point of view, between the $(E_{es} + E_{pl})$ term and the $(E_{ex} + E_{ct})$ term. The E_{es} and E_{pl} components are obtained by neglecting the differential overlap between the atomic orbitals from different monomers. While that, in the calculation of the E_{ex} and E_{ct} components the intermolecular differential overlap between the atomic orbitals is allowed. (Morokuma, K.; Kitaura, K. Energy Decomposition Analysis of Molecular Interactions. In *Chemical Applications of Atomic and Molecular Electronic Potentials*; Politzer, P., Truhlar, D. G., Eds.; Plenum: New York, 1981; p 215.) In consequence, because the atomic orbitals overlap among the monomers, the $(E_{ex} + E_{ct})$ term takes into account the "sharing" of electrons between the monomers and in turn the formation of a bond with some covalent character.

4710

dx.doi.org/10.1021/jp1105168 |*J. Phys. Chem. A* 2011, 115, 4701–4710